

SUPPORTING INFORMATION

Manuscript Title: Camera trapping and spatially explicit capture-recapture for the monitoring and conservation management of lions: insights from a globally important population in Tanzania

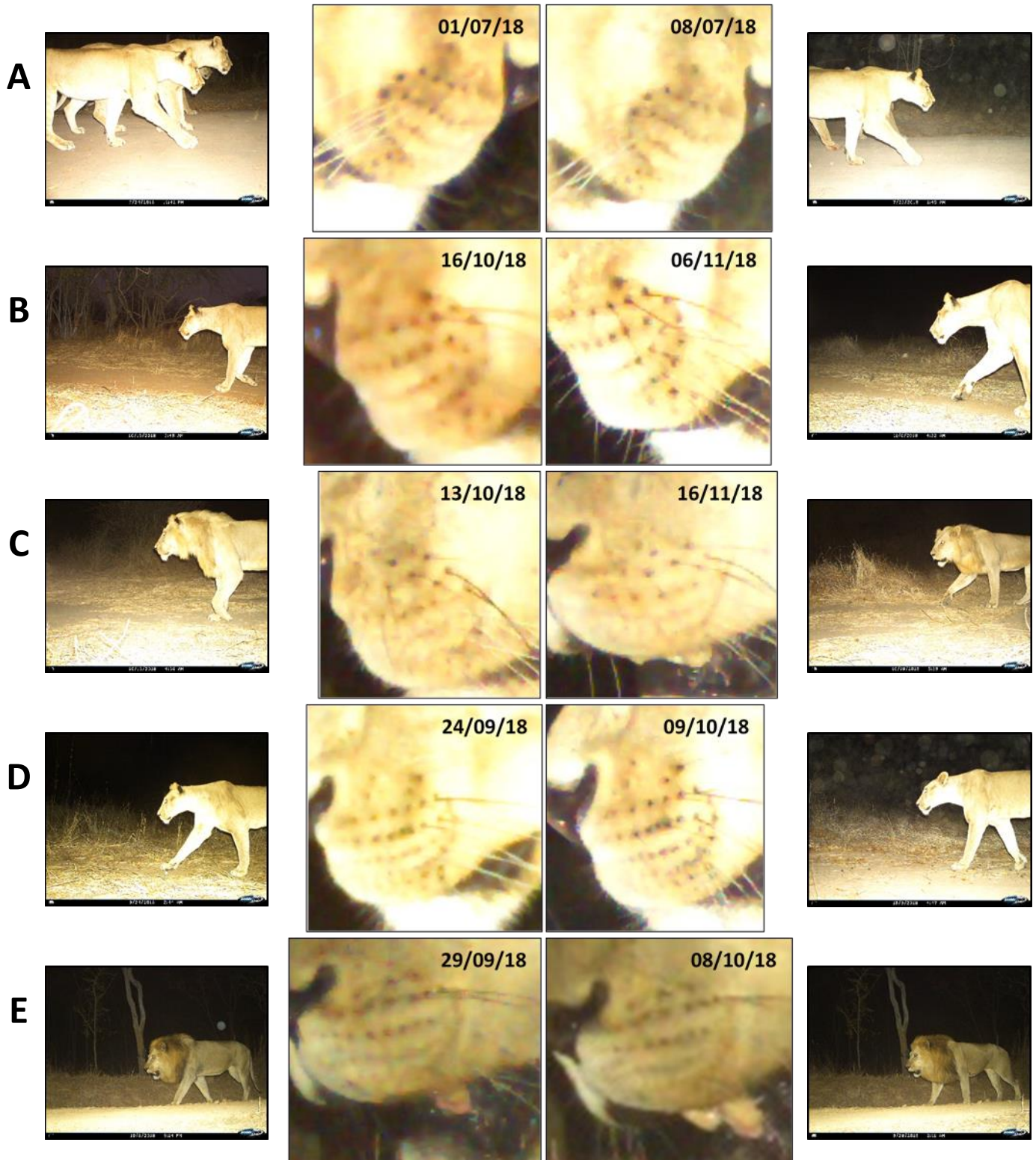
Authors: Paolo Strampelli, Charlotte E. Searle, Josephine B. Smit, Philipp Henschel, Lameck Mkuburo, Dennis Ikanda, David W. Macdonald, Amy J. Dickman

Journal: Ecological Solutions and Evidence

APPENDIX S1 – Additional examples of key lion identification features

Whisker spots

Individual lions exhibit unique combinations of whisker spots. The xenon flash and high quality of the pictures (in turn allowing for considerable magnification) leads to these being visible if the camera is set at an appropriate height and distance from the road or trail. The top and bottom rows, in particular, show a high degree of variation and assist with identification.



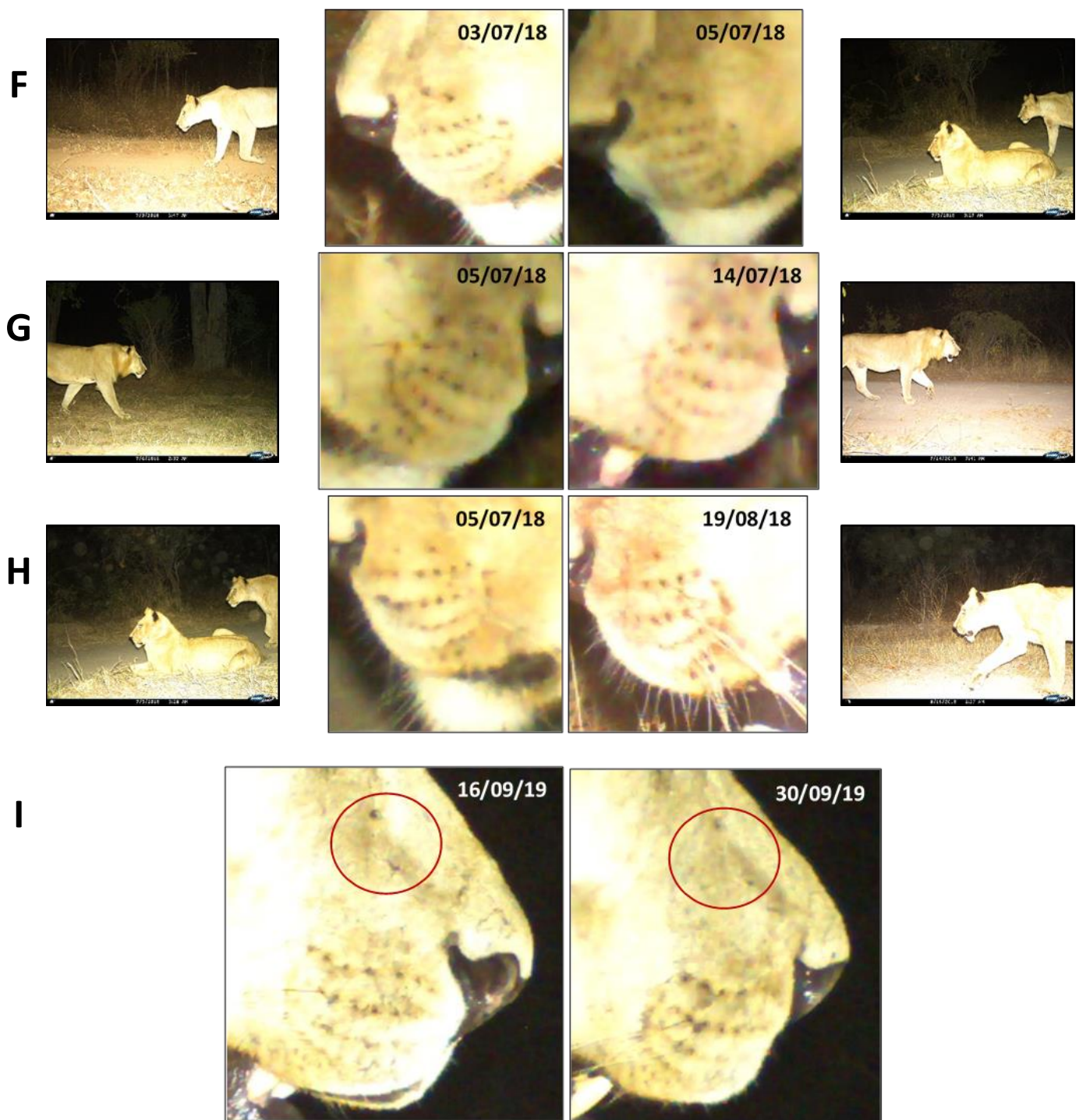


Fig. S1.1: A-H: Examples of whisker spot patterns of lions from camera trap pictures from this study. Even when pictures are slightly overexposed, the dark colour of whisker spots means they are often visible and suitable for identification. I: The high quality of the photographs, and the consequent potential for considerable magnification, results in smaller scars and marks (circled in red), which are often present on the face, also assisting identification.

Scars & Marks

Most individuals exhibited one or more scars or marks that aided identification. These are particularly visible thanks to the xenon flash and the consistent framing. Below we provide examples of different types of scars and marks, and how these can be used to assist with individual identification.

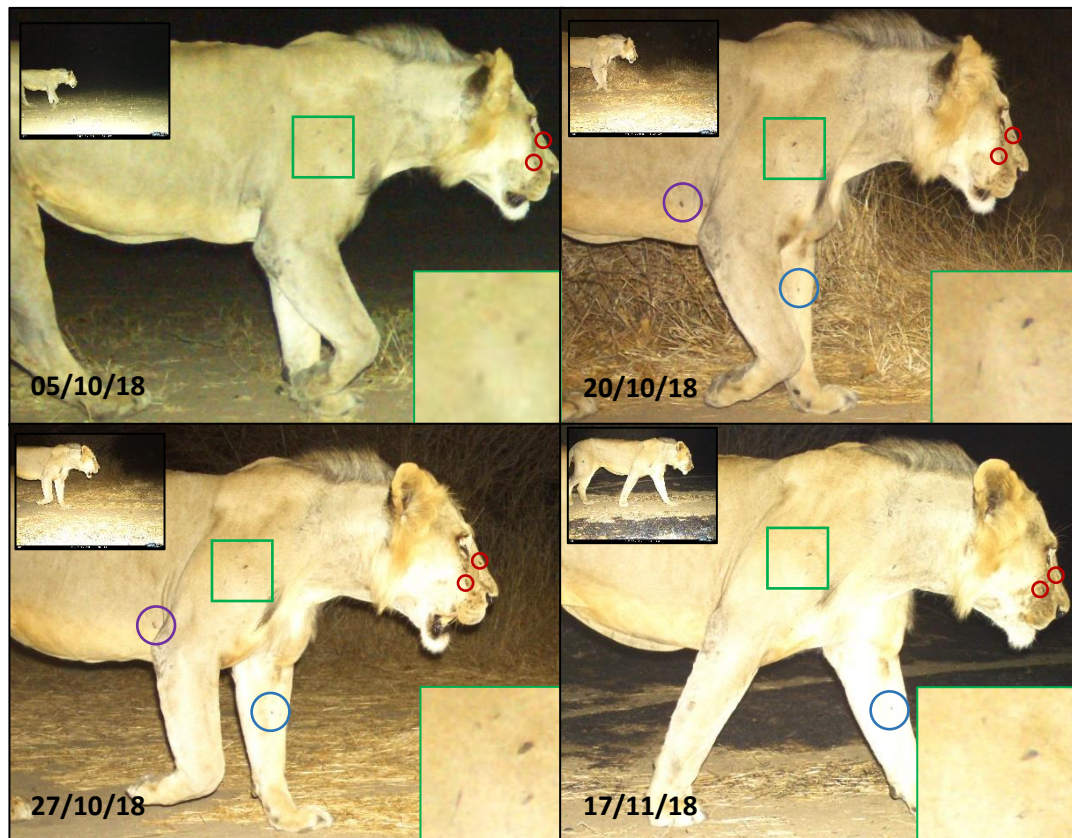


Fig. S1.2: Four pictures of the same male lion, 43 days apart. The xenon flash, consistent framing, and high quality of the pictures allows the identification of a number of characteristic scars and marks. For each capture, the top left inset shows the original picture, while the bottom right inset shows magnified scars on the right leg. Circled areas show additional scars or marks (may require additional magnification). While the absence of a scar or a mark should not be used to exclude individuals (unless the scar or mark is present in captures both before and after the capture of interest), their presence can be used to assist with identification (although their usefulness will be lower for multi-year studies). While whisker spots are less clear in older lions, these are also the individuals which typically exhibit the greatest number of scars and marks.

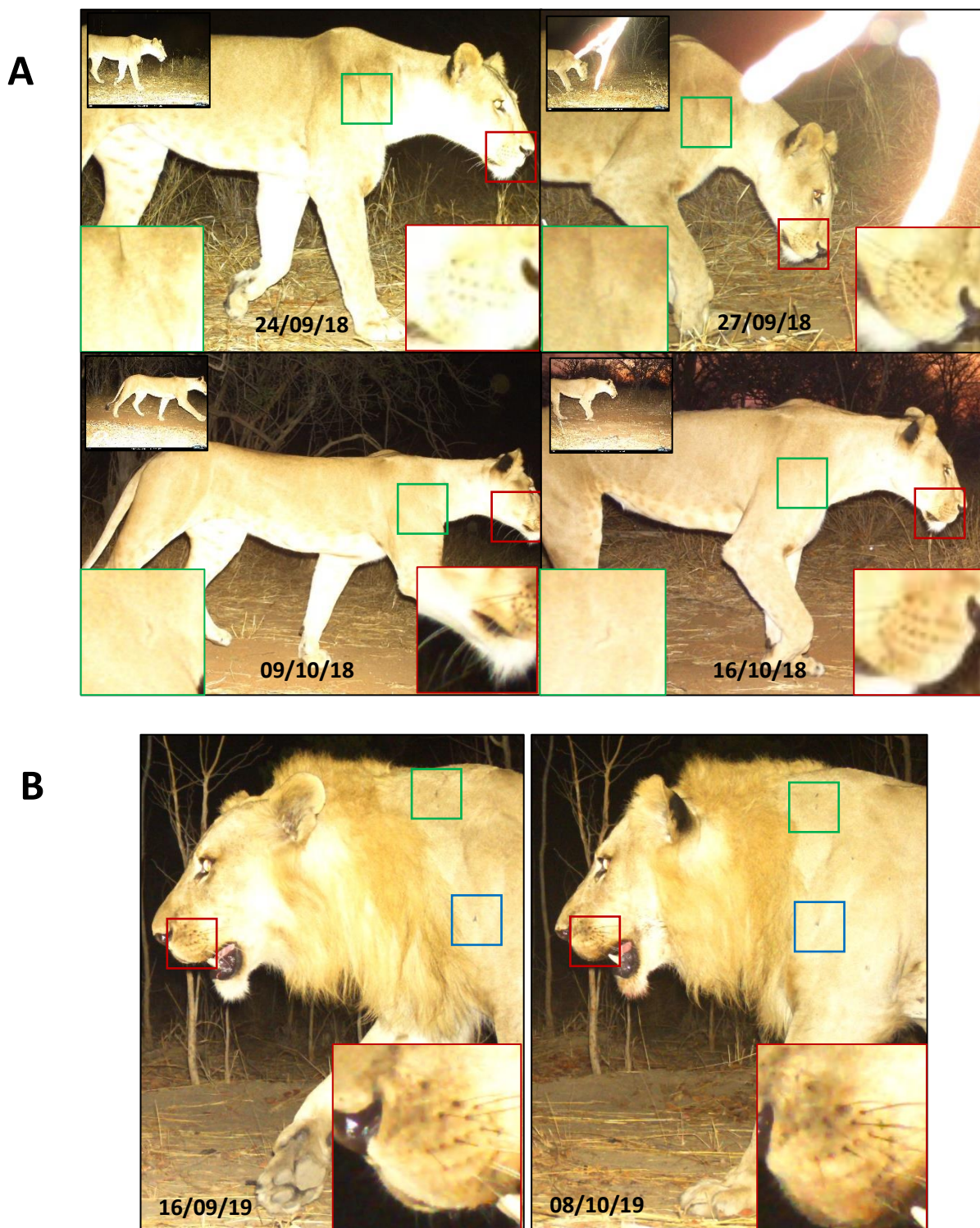


Fig. S1.3: Most individuals were identified from a combination of whisker spots and scars or marks. In the case of this female (A), the presence of a relatively faint but characteristic 'S' shaped mark on the right shoulder meant that, in the event of whisker spots not being visible (as is partly the case in the third capture), it is nevertheless possible to achieve identification (the assumption is made that a separate individual will not exhibit the exact same mark in the exact same location). The similar is true for the male (B), with both whisker spots and the two small scars on the shoulders matching.

A



B



C



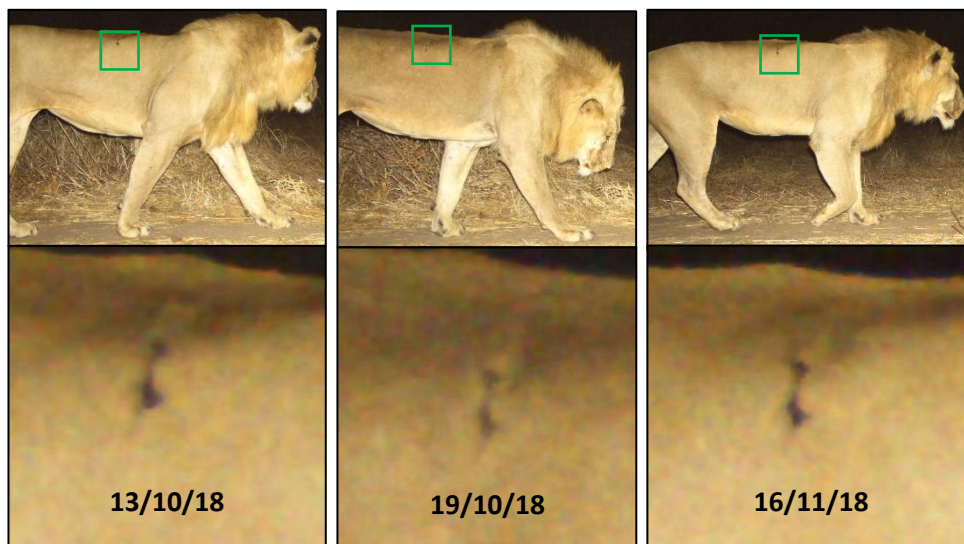
D**E****F**

Fig. S1.4 Most lions will exhibit small scars or marks that, provided consistent framing, the use of a xenon flash, and magnification, can assist identification. Note how these can remain visible for several months.

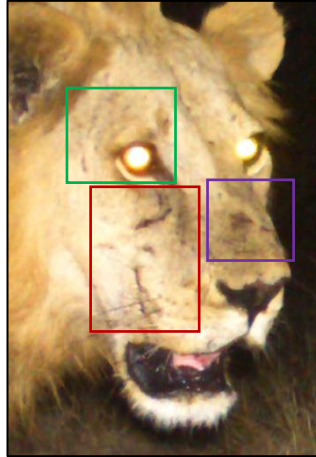
A

23/06/2018



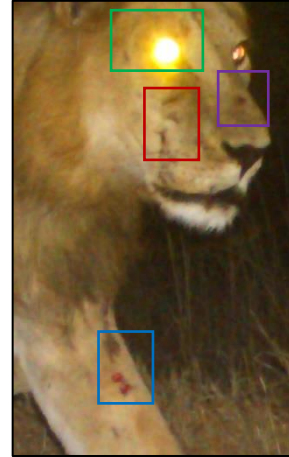
First capture. Scars are visible around the right eye.

20/07/2018



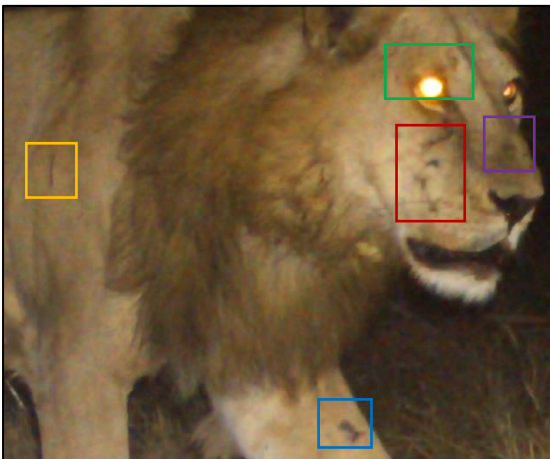
Almost a month later, scars around the eye are still visible. New scars are visible on the right cheek and nose.

22/07/2018



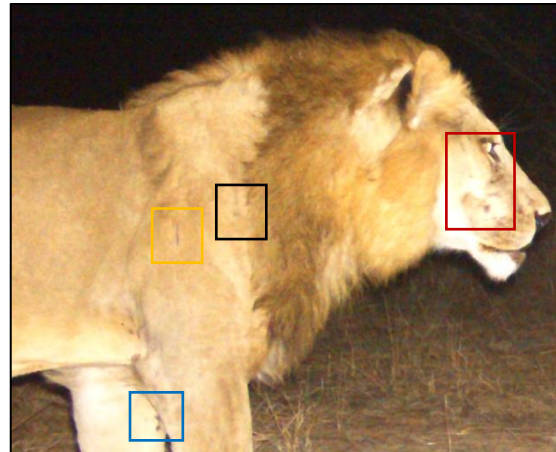
All previous scars are still visible. A new wound on the inner front left leg is now also visible.

04/08/2018



Almost two weeks later, the scars around the eye and on the nose are now faint (but still visible). Scars on the cheek and on the left leg are still visible, and a new scar on the right shoulder is now visible.

18/08/2018



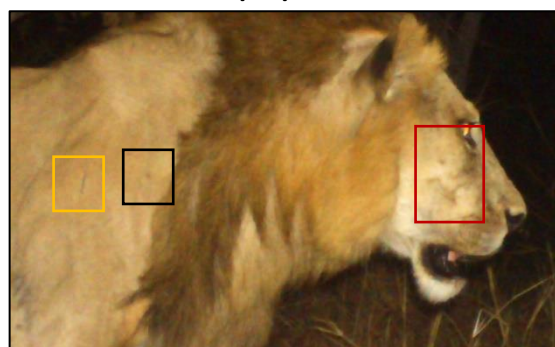
Another two weeks later, the scars on the eye are now very faint, and not reliable for identification. Those on the cheek, shoulder, and inner left leg are still visible and suitable for identification. A small additional scar on the shoulder is now also visible.

28/08/2018



The scar on the cheek, while slightly fainter, is still visible and suitable to assist identification. The other three scars are also still visible.

07/09/2018



Approximately two and a half months from the first capture, all scars are now different from those present then. The fact that new scars often appear to 'replace' fading ones, as seen here, assists considerably with identification.

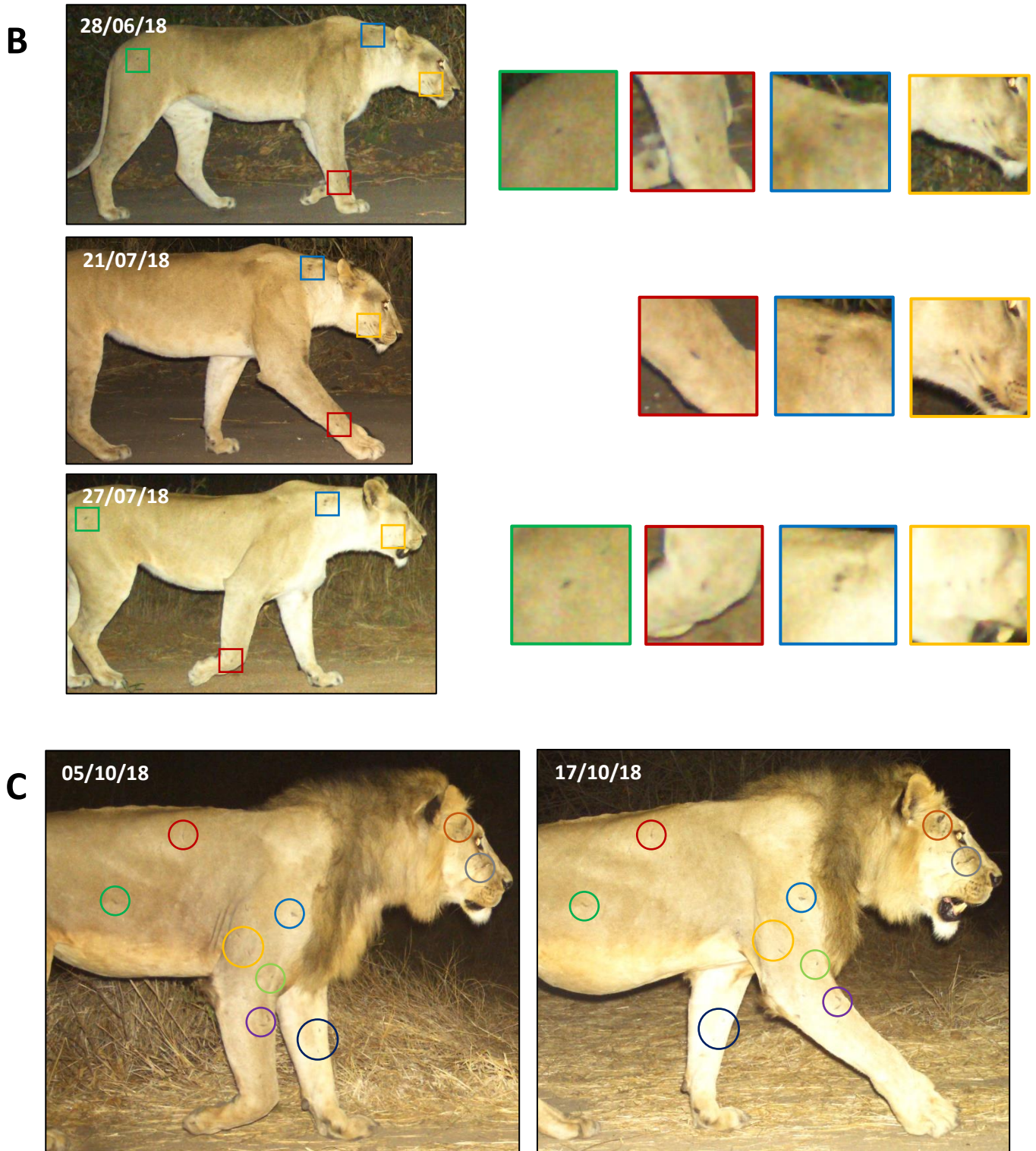


Fig S1.5: Examples of small yet characteristic marks and scars that can assist with individual identification. Most lions captured had at least one such scar or mark, with many having multiple. Note how these can remain visible for several months. A: evolution of scars and marks over time for a male lion in this study. B,C: Individuals with at least four (B) and nine (C) visible scars or marks, respectively. Although some will fade over the course of the survey, some will likely remain for the duration of the survey (or new ones may appear), thus facilitating individual identification.

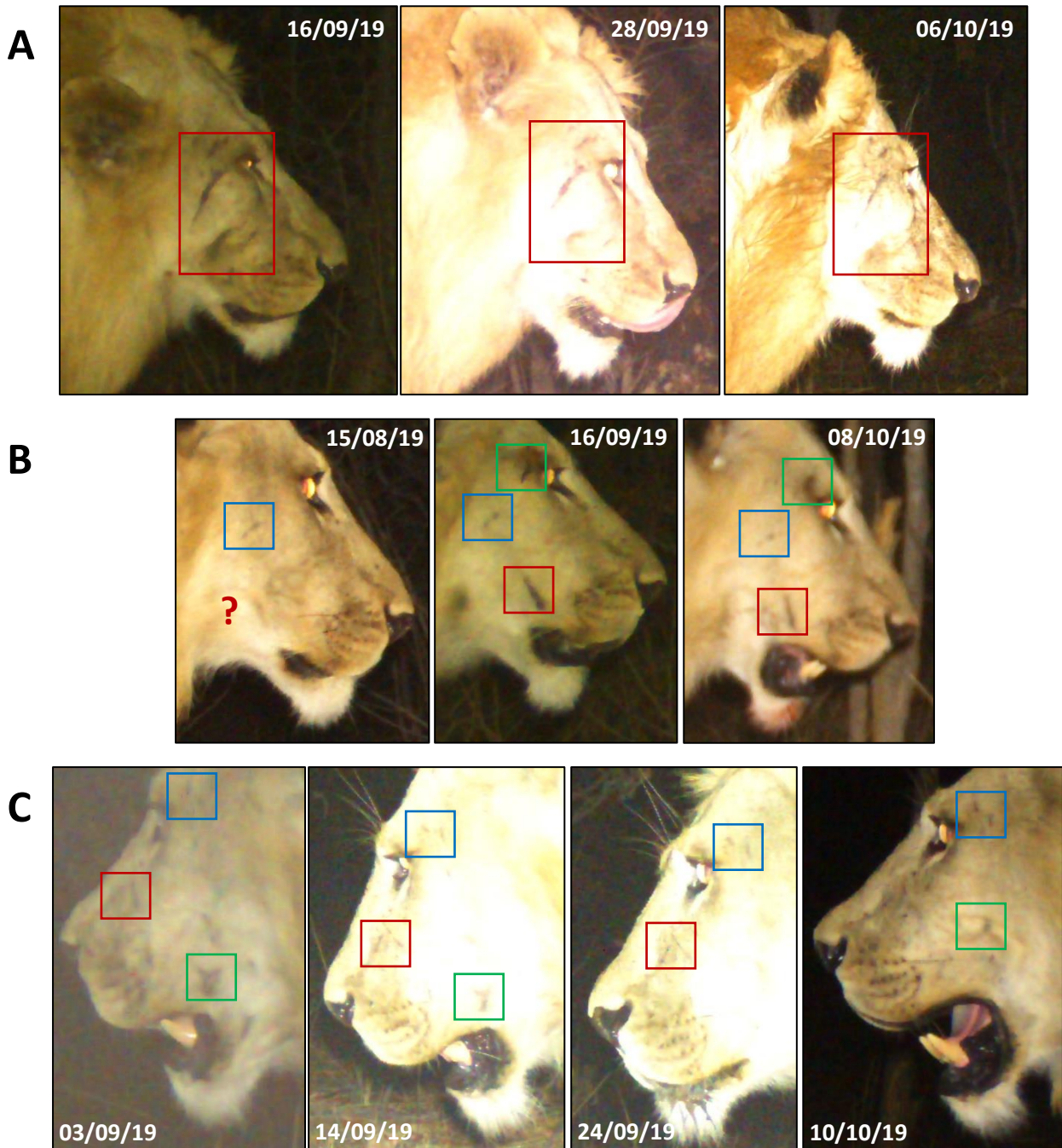


Fig. S1.6: Male lions, in particular, often exhibit characteristic scars on the face. This can lead to individuals being identifiable even if photographs do not depict whisker spots particularly clearly. Note that the second individual (B) only received the scar behind the eye after the 15th of August, and it is unclear whether at this point it already had the scar on the cheek; such temporal information can also be used to facilitate the identification process. In the case of the third individual (C), the presence of three characteristic scars (on the temple, on the nose, and on the cheek), led the first picture to be classified as the same individual, even though picture quality is fairly poor and whisker spots are not visible.

Mane size, colour, and development (males only)

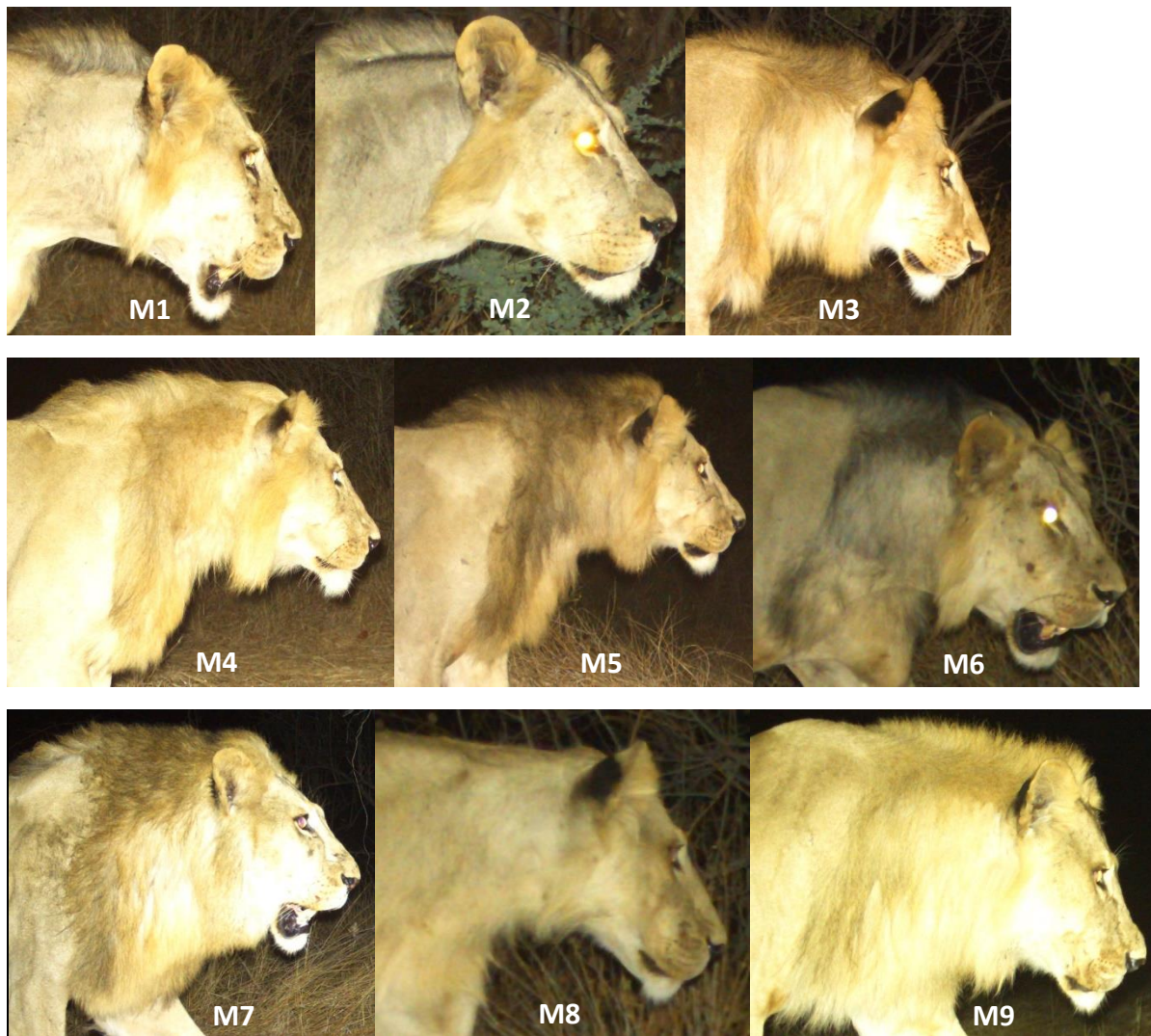


Fig. S1.7: The nine male lions identified in the MBOMIPA WMA camera trap grid.

Male lion mane size, colour, and development also proved useful for individual identification. Fig. S1.7 depicts all nine male lions identified during the MBOMIPA WMA grid survey. As can be seen, except for a few individuals which exhibit similar manes (M1 and M2; M3, M4, and M9; M5 and M7), the mane alone is sufficient to reduce the pool of potential individuals a capture could be depicting before requiring the inspection of finer-scale features (e.g. whisker spots, scars, nose shape). It is also worth noting that differences in mane colour (e.g. between M4 and M5) are due to differences in the manes themselves, and not a result of flash intensities, distance, or time of capture. While manes will change over time, meaning their usefulness for identification will be reduced in multi-year studies, they are nevertheless very useful to increase the efficiency of the identification process.

Knee hair tufts (males only)

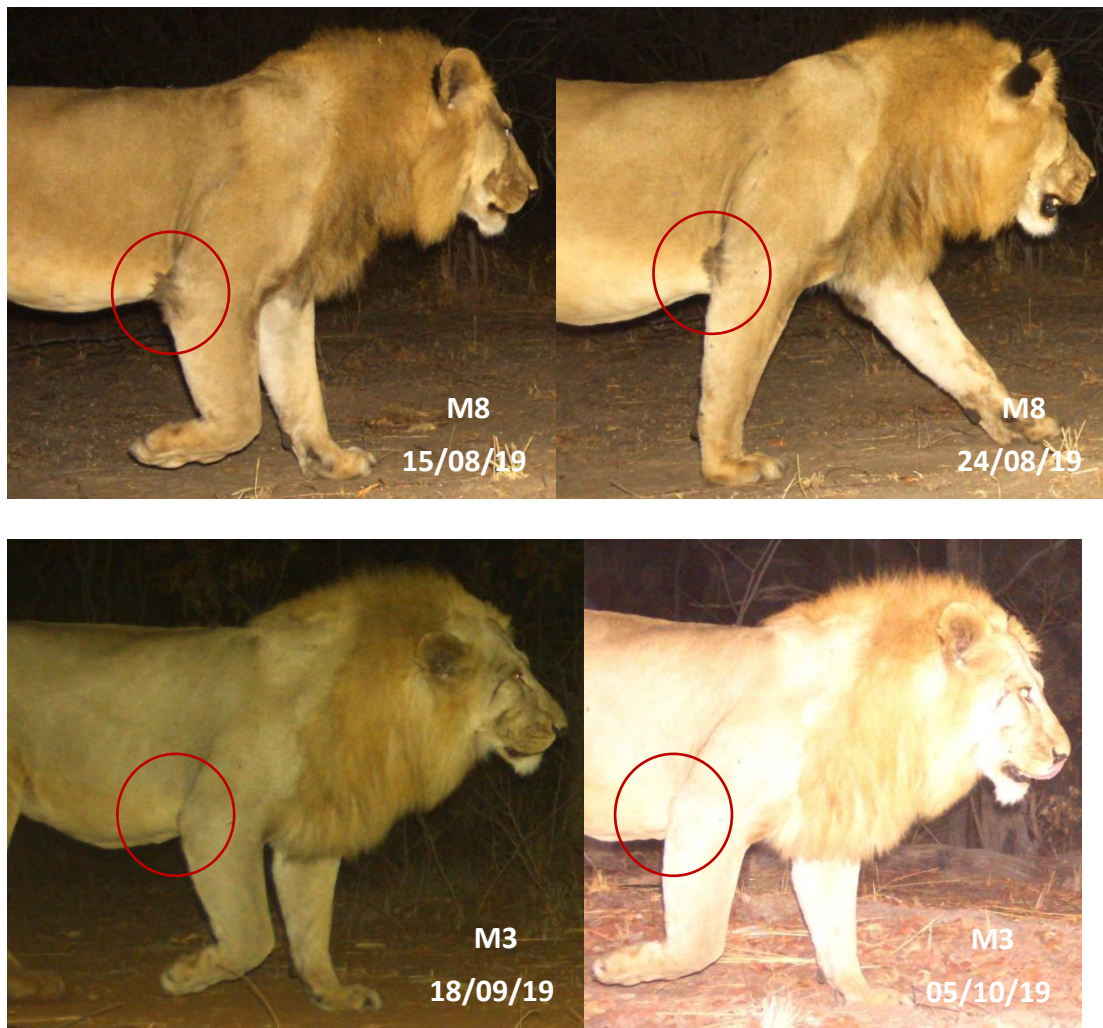


Fig. S1.8: Two male lions in Rungwa GR with similar mane size, development, and colour, but markedly different knee hair tufts.

Knee hair tufts also proved a useful feature to increase the efficiency of the identification process for males, as these – much like manes – varied considerably in size. Fig. S1.8 depicts two males of similar body and mane size and shape from Rungwa GR; however, while M8 has large knee hair tufts, these are completely absent in male M3 (this absence being clearly visible even in the lower-quality second picture).

Nose shape



Fig. S1.9: Two female lions with markedly different nose shapes. Also note the distinctive ear notch on lion R31.

While nose shape was never used as the main identifying feature, due to observed variation between individuals it can be helpful to rapidly eliminate individuals as possible ‘matches’, thus increasing the efficiency of the identification process.

APPENDIX S2 – SECR Input Files

All SECR input files, for all analyses, can be accessed at:

<https://github.com/pstrampelli/SECR-Input-Files>

[DOI: 10.5281/zenodo.5846471](https://doi.org/10.5281/zenodo.5846471)

APPENDIX S3 – Supplementary Tables

Table S3.1 Rankings of models describing lion population density for four survey grids in Ruaha-Rungwa, based on AIC corrected for small sample size (AICc). Top-ranked model shaded in grey.

Model ¹	nPar ²	LogLik ³	AICc ⁴	ΔAICc ⁵	AICc Wt ⁶
Ruaha NP – Core (<i>Acacia-Commiphora</i>)					
secr.road.sex.g	6	-709.4524	1432.954	0.000	0.5366
secr.road.sex	7	-708.2932	1433.386	0.432	0.4324
Secr.road.sex.s	6	-712.3028	1438.654	5.700	0.0310
secr.road	5	-717.3033	1446.035	13.081	0.0000
secr.sex	6	-716.2892	1446.627	13.673	0.0000
secr.sex.g	5	-717.8330	1447.095	14.141	0.0000
secr.sex.s	5	-720.9387	1453.306	20.352	0.0000
secr.0	4	-726.1470	1461.224	28.270	0.0000
Ruaha NP – Woodlands (miombo)					
secr.0	4	-143.5402	299.525	0.000	0.7961
secr.road	5	-143.3846	304.269	4.744	0.0743
secr.sex.s	5	-143.5010	304.502	4.977	0.0661
secr.sex.g	5	-143.5402	304.580	5.055	0.0636
secr.road.sex.s	6	-143.3487	310.697	11.172	0.0000
secr.road.sex.g	6	-143.3841	310.768	11.243	0.0000
secr.sex	6	-143.4991	310.998	11.473	0.0000
secr.road.sex	7	-143.3482	319.363	19.838	0.0000
MBOMIPA WMA (<i>Acacia-Commiphora</i>)⁷					
secr.sex.s	5	-134.4441	283.888	0.000	0.6828
secr.road.sex.s	6	-134.0510	287.738	3.850	0.0996
secr.sex.g	5	-136.4340	287.868	3.980	0.0933
secr.sex	6	-134.1178	287.872	3.984	0.0932
secr.road.sex.g	6	-136.1072	291.851	7.963	0.0127
secr.0	4	-140.5996	292.276	8.388	0.0103
secr.road.sex	7	-133.7871	292.774	8.886	0.0080
secr.road	5	-139.9246	294.849	10.961	0.0000
Rungwa GR (miombo)⁷					
secr.road.sex.s	6	-172.3788	362.758	0.000	0.6539
secr.road.sex	7	-170.7210	364.057	1.299	0.3415
secr.sex	6	-177.3467	372.693	9.935	0.0046
secr.sex.s	5	-180.0976	374.195	11.437	0.0000
secr.road.sex.g	6	-180.0486	378.097	15.339	0.0000
secr.road	5	-182.2076	378.415	15.657	0.0000
secr.sex.g	5	-188.9111	391.822	29.064	0.0000
secr.0	4	-191.3137	393.127	30.369	0.0000

¹ secr.0 = null model; secr.sex = σ and g0 vary with sex; secr.sex.s = σ varies with sex; secr.sex.g = g0 varies with sex; secr.road = g0 varies with station location (on- or off-road); secr.road.sex = g0 varies with station location and sex; σ varies with sex; secr.road.sex.s = g0 varies with station location; σ varies with sex; secr.road.sex.g = g0 varies with station location and sex

² Number of model parameters

³ Log-likelihood

⁴ Akaike Information Criterion, adjusted for small sample size

⁵ Difference from best ranking (lowest AIC) model

⁶ AICc model weights

⁷ For sites with two investigators (MBOMIPA WMA & Rungwa GR), results from the consensus capture histories are presented; see Appendix S4 for the complete model rankings

Table S3.2 Population density parameter estimates for the four survey grids, based on the top-ranked model

secr Model Parameter ¹	Estimate \pm SE	95% CI
Ruahha NP (core)		
<i>g0</i> (F, on-road)	0.014 \pm 0.002	0.012 – 0.017
<i>g0</i> (M, on-road)	0.024 \pm 0.003	0.019 – 0.030
<i>g0</i> (F, off-road)	0.006 \pm 0.001	0.004 – 0.010
<i>g0</i> (M, off-road)	0.011 \pm 0.003	0.007 – 0.017
σ	3584 \pm 174	3259 – 3941
<i>D</i>	6.12 \pm 0.94	4.54 – 8.26
Ruahha NP (miombo)		
<i>g0</i>	0.009 \pm 0.003	0.005 – 0.016
σ	4926 \pm 828	3551 – 6833
<i>D</i>	1.75 \pm 0.62	0.88 – 3.45
MBOMIPA WMA		
Investigator 1		
<i>g0</i>	0.018 \pm 0.004	0.014 – 0.028
σ_F	1670 \pm 206	1313 – 2125
σ_M	2963 \pm 379	2308 – 3804
<i>D</i>	4.05 \pm 1.02	2.49 – 6.60
Investigator 2 & Consensus		
<i>g0</i>	0.017 \pm 0.004	0.011 – 0.028
σ_F	1691 \pm 212	1325 – 2159
σ_M	2995 \pm 394	2317 – 3871
<i>D</i>	4.06 \pm 1.03	2.49 – 6.62
Rungwa GR		
Investigator 1		
<i>g0</i> (on-road)	0.006 \pm 0.001	0.004 – 0.009
<i>g0</i> (off-road)	0.017 \pm 0.004	0.010 – 0.027
σ_F	2682 \pm 337	2099 – 3426
σ_M	5405 \pm 693	4208 – 6944
<i>D</i>	2.74 \pm 0.66	1.72 – 4.35
Investigator 2		
<i>g0</i> (on-road)	0.004 \pm 0.001	0.003 – 0.007
<i>g0</i> (off-road)	0.014 \pm 0.003	0.008 – 0.024
σ_F	3467 \pm 470	2662 – 4516
σ_M	5604 \pm 755	4309 – 7290
<i>D</i>	2.30 \pm 0.54	1.45 – 3.63
Consensus		
<i>g0</i> (on-road)	0.006 \pm 0.001	0.003 – 0.009
<i>g0</i> (off-road)	0.017 \pm 0.004	0.010 – 0.028
σ_F	2603 \pm 352	1999 – 3389
σ_M	5421 \pm 142	4201 – 6988
<i>D</i>	2.50 \pm 0.64	1.53 – 4.08

¹ D = Population density, defined as the number of adult individuals per 100 km²; SE = standard error; CI = confidence interval; *g0* = capture probability at home range-centre; on-road = camera located on road; off-road = camera located off-road; σ = spatial movement parameter related to home range size; F = female; M = male

APPENDIX S4 – Full SECR Model Outputs

Full SECR model outputs, from all analyses, can be accessed at:

<https://github.com/pstrampelli/Full-SECR-Modelling-Outputs>